Geophysical Research Letters

RESEARCH LETTER
10.1029/2026GL121909

Reduced West Antarctic Ice Sheet Size During Prominent Quaternary Interglacials Constrained by Iceberg-Rafted Debris Provenance in the Amundsen Sea

Patric Simões Pereira[1,2], Claus-Dieter Hillenbrand[3], Sidney R. Hemming[4], James W. Marschalek[1], Rob Larter[3], James A. Smith[3], Gerhard Kuhn[5], and Tina van de Flierdt[1]

[1]Department of Earth Science and Engineering & Grantham Institute for Climate Change and the Environment, Imperial College London, London, UK, [2]Institute of Geology, University of Innsbruck, Innsbruck, Austria, [3]British Antarctic Survey, Cambridge, UK, [4]Lamont-Doherty Earth Observatory of Columbia University, Palisades, New York, NY, USA, [5]Alfred-Wegener-Institut Helmholtz-Zentrum für Polar- und Meeresforschung, Bremerhaven, Germany

Key Points:

- Contrasting glacial-interglacial iceberg-rafted debris (IRD) provenance changes between PC493 and PS58/254 reflect latitudinal shifts in ocean current boundaries
- Abundant <10 Ma-old grains during MIS 5, 11, and 15 at site PS58/254 indicate a reduced West Antarctic Ice Sheet elevation
- The absence of East Antarctic debris in the Amundsen Sea is consistent with limited or partial retreat of the West Antarctic Ice Sheet

Supporting Information:

Supporting Information may be found in the online version of this article.

Correspondence to:

P. Simões Pereira,
patric.simoes-pereira@uibk.ac.at

Citation:

Simões Pereira, P., Hillenbrand, C.-D., Hemming, S. R., Marschalek, J. W., Larter, R., Smith, J. A., et al. (2026). Reduced West Antarctic Ice Sheet size during prominent Quaternary interglacials constrained by iceberg-rafted debris provenance in the Amundsen Sea. *Geophysical Research Letters*, *53*, e2026GL121909. https://doi.org/10.1029/2026GL121909

Received 21 JAN 2026
Accepted 9 JUN 2026

Author Contributions:

Conceptualization: Patric Simões Pereira, Claus-Dieter Hillenbrand, Tina van de Flierdt
Data curation: Patric Simões Pereira
Formal analysis: Patric Simões Pereira
Funding acquisition: Tina van de Flierdt
Investigation: Patric Simões Pereira, Sidney R. Hemming
Resources: Claus-Dieter Hillenbrand, Sidney R. Hemming, Rob Larter, James A. Smith, Gerhard Kuhn, Tina van de Flierdt

Abstract The stability of the West Antarctic Ice Sheet (WAIS) remains a major uncertainty in sea-level projections, and geologic records provide important constraints on its past behavior. We present $^{40}Ar/^{39}Ar$ ages of biotite and hornblende grains from iceberg-rafted debris (IRD) in two Amundsen Sea sediment cores (PC493 and PS58/254), located south and north of the southern boundary of the Antarctic Circumpolar Current (sbACC), respectively. Over the past 850,000 years, PC493 records a stable IRD provenance dominated by eastern Amundsen Sea sources, consistent with transport by the westward-flowing Antarctic Coastal Current. In contrast, PS58/254 shows temporally variable sources, with southeastern Amundsen Sea inputs during glacials and increased Marie Byrd Land contributions during interglacials, indicating latitudinal sbACC shifts. The absence of East Antarctic IRD is consistent with no open-marine connection between the Weddell and Amundsen Seas, while abundant <10 Ma grains during Marine Isotope Stages 5, 11, and 15 imply reduced WAIS elevation.

Plain Language Summary The stability of the West Antarctic Ice Sheet is a major uncertainty in predicting future sea-level rise. To understand how one of its most sensitive regions behaved in the past, we studied minerals carried by icebergs and deposited in ocean sediments from two sites in the Amundsen Sea. These minerals can be linked to specific rocks on land, allowing us to track iceberg sources over the past 850,000 years. Site PC493 shows a consistent source of material, suggesting a long-lasting westward-flowing ocean current along the Antarctic coast. In contrast, site PS58/254 shows changes in sediment sources between colder and warmer periods, indicating shifts in ocean circulation. We find no evidence that the ocean was ever fully open between East and West Antarctica. This suggests that a complete collapse of the West Antarctic Ice Sheet is unlikely. However, higher abundances of young rock fragments during several warm periods indicate that the ice sheet was at a lower elevation than today. A thinner ice sheet likely exposed volcanic rocks, which were then broken down by erosion, rockfalls, and moraine formation, and carried offshore by glaciers. These findings improve understanding of past ice sheet behavior and help refine predictions of future sea-level rise.

1. Introduction

Detrital $^{40}Ar/^{39}Ar$ ages obtained from coarse (>63 μm) biotite and hornblende grains in iceberg-rafted debris (IRD) of Southern Ocean sediments offer a valuable method for inferring the glacial variability of specific Antarctic Ice Sheet (AIS) drainage sectors during periods of past warmth (Pierce et al., 2014; Roy et al., 2007; Simões Pereira et al., 2018, 2020). Age populations derived from such analyses allow determination of IRD provenance by matching these to cooling ages of potential source rocks on the Antarctic continent, hence informing on the location of active glacial erosion and ice discharge through iceberg calving. To date, no study has specifically investigated downcore provenance changes using $^{40}Ar/^{39}Ar$ ages of biotite and hornblende grains from sediment archives in the Amundsen Sea to reconstruct late Quaternary dynamics of the West Antarctic Ice Sheet (WAIS). The marine-based parts of the WAIS contain ice with the potential to raise global sea-level by 3.3 m and are considered inherently unstable because much of this ice rests on a retrograde bed below sea level (Morlighem et al., 2020). The Amundsen Sea lies directly offshore from the most vulnerable WAIS drainage sector, where today two major outlets, the Pine Island and Thwaites Glaciers, are experiencing the largest amount

Supervision: Claus-Dieter Hillenbrand, Tina van de Flierdt
Visualization: Patric Simões Pereira
Writing – original draft: Patric Simões Pereira
Writing – review & editing: Patric Simões Pereira, Claus-Dieter Hillenbrand, Sidney R. Hemming, James W. Marschalek, Rob Larter, James A. Smith, Gerhard Kuhn, Tina van de Flierdt

of ice loss in Antarctica (Rignot et al., 2019). Both ice streams are inferred to have significantly retreated or even completely disintegrated during late Quaternary interglacials based on ice-sheet modeling (DeConto & Pollard, 2016; Golledge et al., 2021; Sutter et al., 2019), micropaleontologic and cosmogenic nuclide data from modern tills elsewhere in Antarctica (Scherer et al., 1998) and genetic data of Antarctic octopuses (Lau et al., 2023). Critical evidence constraining the timing and extent of glacial retreat upstream into the West Antarctic interior remains largely absent from the Amundsen Sea sector. Here, we present $^{40}Ar/^{39}Ar$ ages from iceberg-rafted biotite and hornblende grains in two sediment cores from the Amundsen Sea continental margin which record glacial-interglacial cycles since the Mid-Pleistocene. These data permit tracking of changes in IRD provenance and therefore reconstruction of changes in ocean circulation and sediment source regions in response to WAIS change.

2. Geological Setting and Source Areas for Glaciogenic Detritus

West Antarctica preserves an extensive, though spatially variable, record of Phanerozoic arc-related magmatism and sedimentation (Jordan et al., 2020). Rock exposures along the Amundsen Sea coast consist predominantly of Paleozoic (~400 Ma) to Cretaceous (~95 Ma) granitoids, with the distinction that the western Amundsen Sea coast notably lacks ~125–240 Ma old plutons. The geology of the Antarctic Peninsula represents a continuation of this arc magmatism, although main calc-alkaline magmatic activity ceased there later, occurring from ~270 Ma to 20 Ma. The region shifted from a convergent to a passive margin before its western part evolved into a rift-dominated setting. The latter stage is recorded by the widespread Miocene to Quaternary volcanic rocks that crop out in different sectors on the continent but are predominantly concentrated within the Marie Byrd Land volcanic province.

Detrital $^{40}Ar/^{39}Ar$ age populations in modern ice-proximal marine surface sediments reflect these geological units, primarily recording ages spanning the Paleozoic to Cenozoic (Simões Pereira et al., 2018, 2020). Crucially, the geology beneath major ice streams draining into the Amundsen Sea Embayment, and more broadly across West Antarctica into the Pacific sector of the Southern Ocean, is sufficiently heterogeneous to distinguish drainage sectors based on distinct detrital signatures (Figure S1 in Supporting Information S1). This heterogeneity enables tracking of sediment sources across key sectors, including the western Antarctic Peninsula, Bellingshausen Sea, Thurston Island, Cosgrove Ice Shelf catchment area, Pine Island Glacier-Thwaites Glacier, western Amundsen Sea Embayment (ASE-W), Wrigley Gulf-Hobbs Coast, and Sulzberger Bay sectors (see Figure S1 in Supporting Information S1 for endmember sample selection). While both Thurston Island and the Cosgrove Ice Shelf catchment areas belong to the same Thurston Island crustal block, distinct age populations reflect basement heterogeneity, with Cretaceous rocks primarily eroded in Cosgrove Ice Shelf's confined catchment, whereas Thurston Island supplies detritus with a broader Paleozoic signal (Figure S1 in Supporting Information S1).

3. Sample Sites and Methods

$^{40}Ar/^{39}Ar$ data were collected from iceberg-rafted biotite and hornblende grains in sediments deposited at two core sites in the Amundsen Sea during glacial and interglacial periods over the past ~850 kyr. Piston core PC493 was retrieved during RRS *James Clark Ross* expedition JR179 (71°08′S, 119°55′W, water depth 2,077 m) in 2008 (Figure 1). The site is strategically located on a seamount on the western Amundsen Sea continental slope and south of the present-day southern boundary of the eastward-flowing Antarctic Circumpolar Current (sbACC). It remained unaffected by turbidity and bottom currents, preserving a condensed but undisturbed and continuous sedimentary sequence of foraminiferal oozes and foraminifera-bearing sandy muds during the last 850 kyr (Williams et al., 2019).

Piston core PS58/254 was collected from the upper continental rise in the eastern Amundsen Sea (69°19′S, 108°27′W, water depth 4,014 m) during RV *Polarstern* cruise ANT-XVIII/5a in 2001. The site is situated on the western flank of a sediment drift north of the sbACC. The upper 15 m of the core comprise alternating diatom-rich muds, diatomaceous oozes, and lithogenic muds (Figure 1) spanning the last 850 kyr (Hillenbrand et al., 2009; Konfirst et al., 2012).

Biotite grains were isolated from the coarse sediment fraction (>63 μm) by sieving and hand-picking, and $^{40}Ar/^{39}Ar$ thermochronological ages were determined at the Argon Geochronology for the Earth Sciences (AGES) Laboratory at Lamont-Doherty Earth Observatory, NY (Supporting Information S1). We consider all detrital sand grains analyzed from cores PC493 and PS58/254 to have been supplied by icebergs. While site

10.1029/2026GL121909

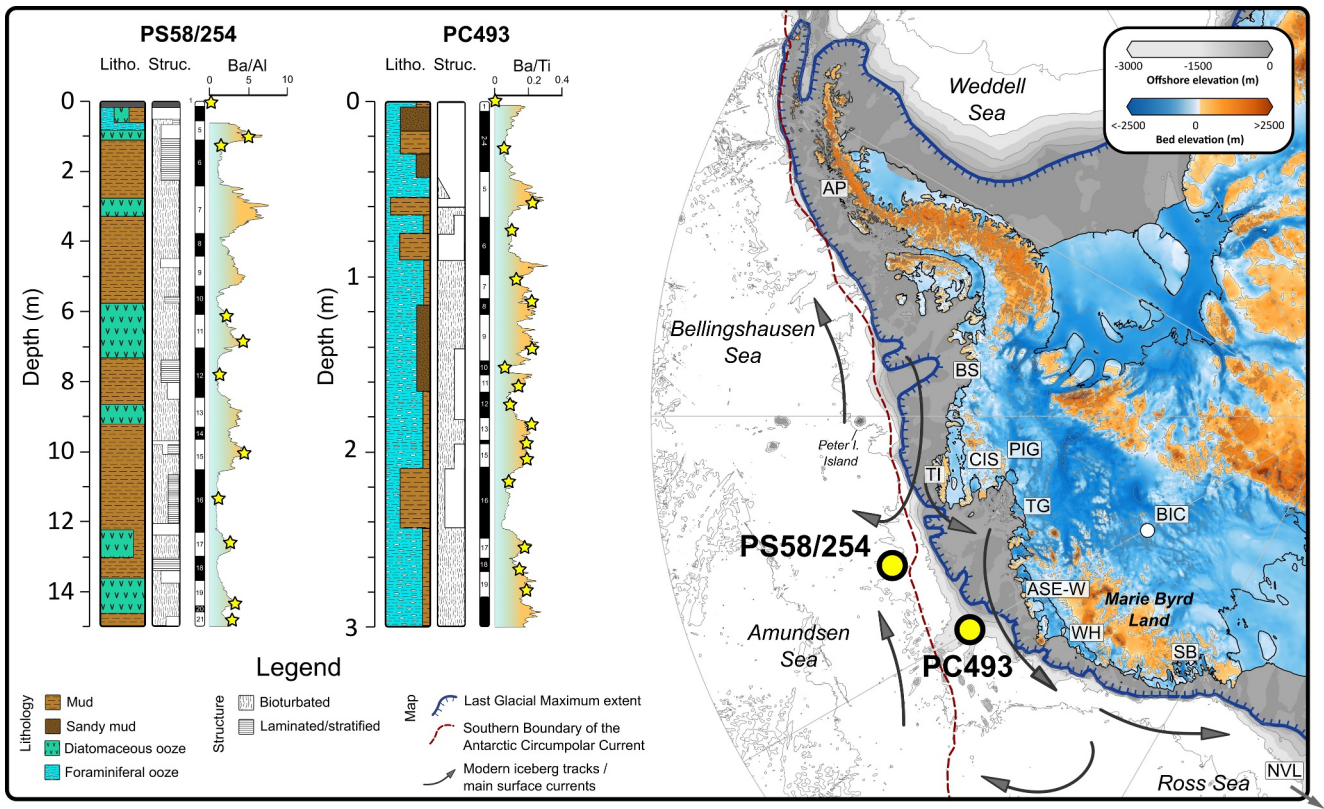

Figure 1. Core logs of PS58/254 and PC493 showing lithology, sedimentary structures, and Ba/Al and Ba/Ti ratios with depth, respectively (Hillenbrand et al., 2009; Williams et al., 2019). Yellow stars mark IRD sampling interval. Right panel shows bed topography below the West Antarctic Ice Sheet (Morlighem et al., 2020) and bathymetry (Dorschel et al., 2022) with sediment core locations (yellow dots), Last Glacial Maximum extent of grounded ice (blue line) (The RAISED Consortium et al., 2014), and the southern boundary of the Antarctic Circumpolar Current (red dashed line) (Orsi et al., 1995). Black arrows indicate modern iceberg tracks (England et al., 2020; Mazur et al., 2019), which generally follow surface currents in the Pacific sector of the Southern Ocean (Holland & Kwok, 2012). ASE-W—Western Amundsen Sea Embayment, AP—Antarctic Peninsula, BIC—Byrd Ice Core (white dot), BS—Bellingshausen Sea, CIS—Cosgrove Ice Shelf, NVL—northern Victoria Land, PIG—Pine Island Glacier, SB—Sulzberger Bay, TG—Thwaites Glacier, TI—Thurston Island, WH—Wrigley Gulf-Hobbs Coast.

PC493 was protected from the deposition of sandy turbidites and the formation of coarse-grained lag deposits by bottom-current winnowing because of its seamount location, the sediments in core PS58/254 consist of terrigenous and diatom-bearing silty clay with extremely rare, thin sand layers, which were avoided for the sampling. The positive correlation between sand and gravel (>2 mm) contents (Hillenbrand et al., 2009) and the scattered distribution of sand and gravel grains in coarser sediment intervals, also document that the detrital sand fraction in core PS58/254 results from IRD delivery. From core PC493, one sample was analyzed for each interglacial and glacial Marine Isotope Stage (MIS), covering MIS 3 to 19 (excluding MIS 4). For core PS58/254, six interglacial (MIS 5, 11, 15, 17, 19, and 21) and four glacial (MIS 6, 10, 12, and 16) samples were analyzed. In addition to the biotite grains, hornblende grains (>150 μm) were picked from samples of core PS58/254, and grains from multiple samples within the same MIS were amalgamated to increase grain numbers and enhance statistical robustness (Supporting Information S1). In total, 307 biotite grains were analyzed from the sandy sediments at site PC493, while the muddy sediments at site PS58/254 yielded a total of 195 grains, comprising 102 biotite and 93 hornblende grains. Data from these records are compared with seafloor surface sediment (MIS 1) samples from box core BC492 (same site as PC493) and PS58/254 previously reported by Simões Pereira et al. (2018).

4. Results

The $^{40}Ar/^{39}Ar$ biotite ages from core PC493 range from ~1 Ma to 315 Ma, with most grains clustering between ~80 Ma and 260 Ma, and three grains yielding older ages between 466 Ma and 495 Ma (Figure 2; see Figure S2 in Supporting Information S1 for detailed distributions). Individual samples display a pronounced peak at ~100 Ma,

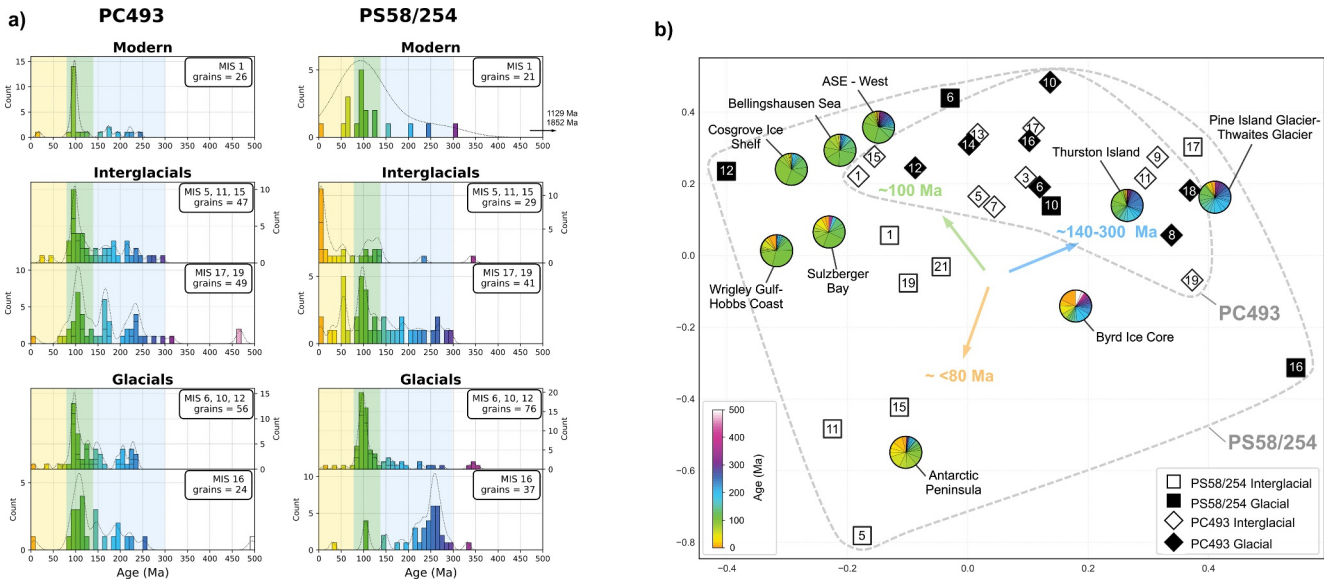

Figure 2. (a) Stacked age histograms and kernel density plots for $^{40}Ar/^{39}Ar$ ages from modern (Simões Pereira et al., 2018), and grouped interglacial and glacial iceberg-rafted grains from sites PC493 and PS58/254. Only samples from equivalent Marine Isotope Stages (MIS) at both sites are shown. Shaded bands highlight key age populations (<80 Ma, ∼100 Ma, 140–300 Ma). (b) Multidimensional scaling (MDS) plot based on the Kolmogrov-Smirnov distance of the individual samples from PC493 (diamonds; biotite), PS58/254 (squares; biotite and hornblende) and West Antarctic source sectors (pie charts displaying $^{40}Ar/^{39}Ar$ biotite and hornblende ages; cf. Figure S1 in Supporting Information S1). Numbers indicate MIS, and sample distributions trend toward the major age populations identified in panel (a).

with additional age clustering between 140 and 260 Ma. Glacial and interglacial populations are broadly similar, except that nearly all grains >260 Ma (n = 9/10) occur during interglacials. Downcore samples from PC493 display age distributions similar to MIS 1, although the latter shows a more prominent peak at 100 Ma than other MIS.

In core PS58/254, biotite and hornblende $^{40}Ar/^{39}Ar$ ages range from ∼1 to 355 Ma (Figure 2; see Figure S3 in Supporting Information S1 for detailed distributions). Biotite and hornblende age distributions are broadly similar within the same samples, except for a distinct ∼60 Ma hornblende population (Supporting Information S1). Previous studies of IRD in seafloor surface sediments from the West Antarctic margin have demonstrated minor mineralogical and thermochronological biases between biotite and hornblende age distributions (Simões Pereira et al., 2018, 2020). Given these similarities and insufficient grain abundances for robust mineral-specific analyses, biotite and hornblende data sets for PS58/254 are interpreted collectively in the following discussion. Unlike PC493, PS58/254 displays significant temporal variations. Interglacial samples from MIS 5, 11, and 15 contain numerous grains younger than 10 Ma and are largely lacking grains >140 Ma. The population of interglacial grain ages from MIS 17, 19, and 21 resembles that of MIS 1, including dates spanning 140–300 Ma. In contrast to the interglacial samples, glacial samples from core PS58/254 contain only very few grains <80 Ma. The ages of grains deposited during glacials also exhibit great variability, with MIS 16 showing a prominent peak at ∼260 Ma, MIS 12 displaying a single peak at ∼100 Ma, while MIS 10 and 6 feature a peak at ∼100 Ma, with ages scattering between 140 and 360 Ma.

5. Discussion

5.1. IRD Provenance Changes Throughout the Last 850 kyr

Multidimensional scaling (MDS) analysis based on Kolmogorov-Smirnov distances (Supporting Information S1) between $^{40}Ar/^{39}Ar$ age populations illustrates distinct provenance patterns between cores PC493 and PS58/254 (Figure 2). In core PC493, interglacial and glacial samples show little internal variation and cluster between the Thurston Island and Pine Island Glacier-Thwaites Glacier endmembers, and the ASE-W, Bellingshausen Sea, and Cosgrove Ice Shelf endmembers (Figure 2, Figure S1 in Supporting Information S1). The former sectors are characterized by biotite age populations with roughly equal abundance, peaking at ∼100 Ma and 140–300 Ma, whereas the latter sectors are dominated by a single ∼100 Ma peak. This supports previous findings by Simões

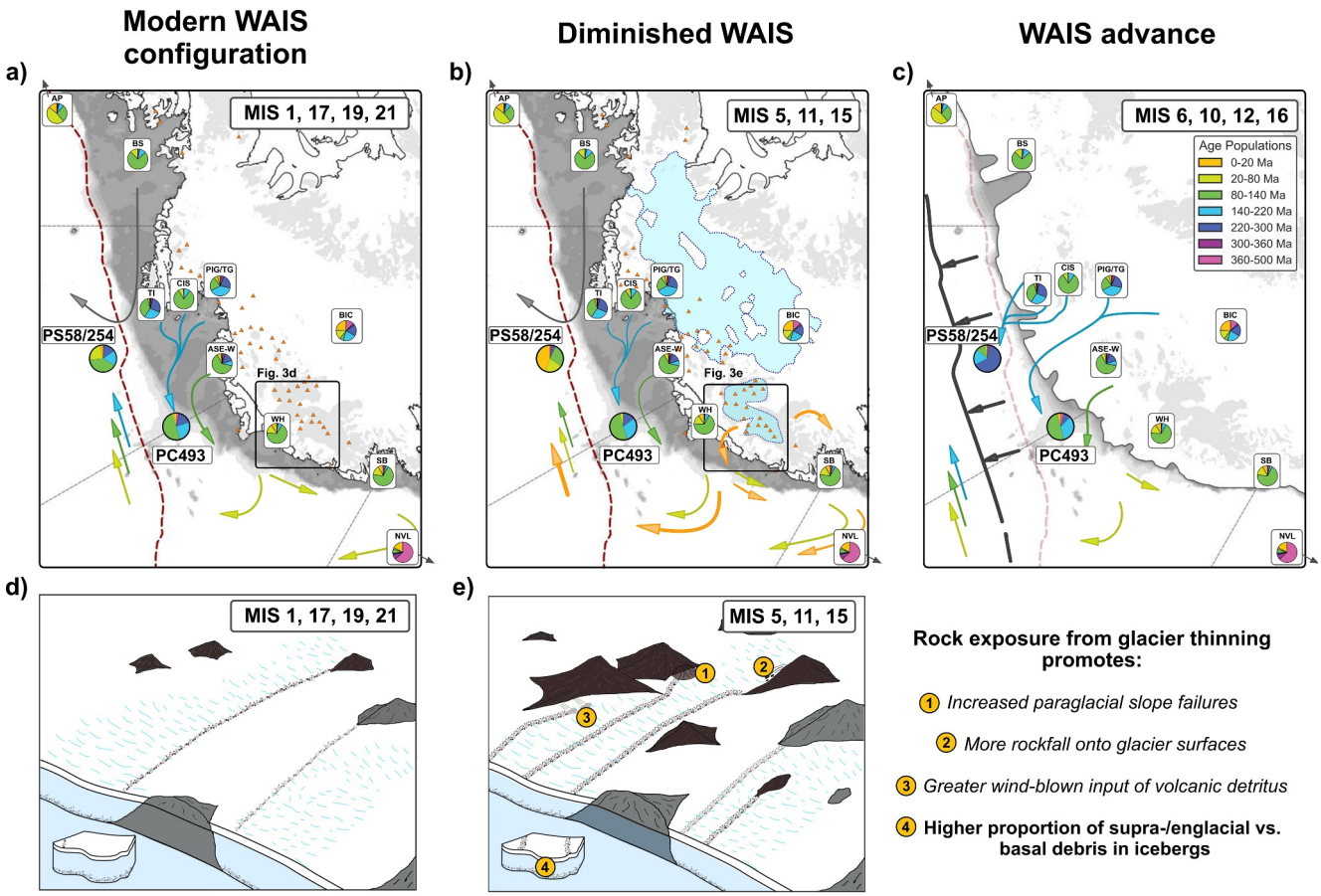

Figure 3. Conceptual models of IRD provenance under different WAIS configurations (a–c), and present glacier setting (d) and a WAIS thinning scenario (e) in Marie Byrd Land. Colored arrows denote surface ocean currents and iceberg pathways. Pie charts denote $^{40}Ar/^{39}Ar$ ages of grains from PC493 (biotite) and PS58/254 (biotite and hornblende) grouped by MIS, and from ice-proximal seafloor surface sediments (hornblende and biotite, cf., Figure S1 in Supporting Information S1). Blue shading marks maximum possible ice retreat in the Pine Island Glacier-Thwaites Glacier sector inferred from the $^{40}Ar/^{39}Ar$ thermochronological ages at sites PC493 and PS58/254 (cf. Golledge et al., 2021), and WAIS thinning across Marie Byrd Land. Red dashed line (left/middle panel) marks the southern boundary of the Antarctic Circumpolar Current (sbACC); black arrows (right panel) show its northward migration during glacial stages. Orange triangles mark volcanic edifices (van Wyk de Vries et al., 2018). Acronyms as in Figure 1.

Pereira et al. (2018), who attributed present-day IRD at site PC493 and nearby sample locations to delivery from eastern Amundsen Sea Embayment sectors, as well as ASE-W sources, via the westward-flowing Antarctic Coastal Current. The ASE-W sector likely supplied more IRD to site PC493 during MIS 1, 12, and 15 compared to other stages, but whether this contribution was intermittent cannot be resolved by our data set.

In contrast, site PS58/254 exhibits a greater provenance variability throughout the record. Interglacial samples from MIS 1, 19, and 21 show similar age populations, plotting between the Thurston Island and Wrigley Gulf-Hobbs Coast sectors in the MDS space, suggesting northward IRD supply from Thurston Island and IRD delivery from Wrigley Gulf-Hobbs Coast by icebergs that were injected from the Antarctic Coastal Current into the ACC in the eastern Ross Sea (Figure 1; England et al., 2020). The Wrigley Gulf-Hobbs Coast source differs from the ASE-W source by a higher proportion of Neogene (<10 Ma) hornblende and ~60 Ma-old biotite grains (Figure 3, Figure S1 in Supporting Information S1), with the latter age peak being prominently present in samples from all three interglacials. The ~60 Ma age peak is absent in bedrock exposed in the Wrigley Gulf-Hobbs Coast sector but may reflect a hidden granitic or dioritic source in Marie Byrd Land, as suggested by apatite fission track ages of Holocene IRD sampled offshore from this sector (Spiegel et al., 2016). Although absent in hornblende grains from the Wrigley Gulf-Hobbs Coast sector, this peak appears in hornblende grains from Sulzberger Bay further west, suggesting IRD could have been entrained into the ACC and transported eastwards to site PS58/254 during MIS 1 and 19, and possibly other interglacials (though no hornblende grains from MIS 17 and 21 were dated). Alternatively, these ~60 Ma ages could derive from parts of the Antarctic Peninsula, although this cannot be

confirmed given the limited grain numbers. While the position of the MIS 17 sample in the MDS space clearly indicates IRD supply from Thurston Island and possibly Pine Island Glacier-Thwaites Glacier, only nine grains were dated from this sample, so other distal sources (such as the Wrigley Gulf-Hobbs Coast sector) cannot be ruled out with confidence.

In contrast to other interglacials at site PS58/254, samples deposited during MIS 5, 11, and 15 plot toward the Antarctic Peninsula source sector due to the higher presence of grains younger than 80 Ma, particularly younger than 10 Ma (Figure 2, Figure S3 in Supporting Information S1). Modern surface sediments from the Bellingshausen Sea shelf, through which Antarctic Peninsula-derived icebergs must pass before reaching the Amundsen Sea, contain only a few <10 Ma grains (Figure S1 in Supporting Information S1), arguing against a significant Antarctic Peninsula contribution to site PS58/254. This is further supported by the tendency of most icebergs calved along the western Antarctic Peninsula and Bellingshausen Sea coasts to enter the ACC north of Thurston Island (Hillenbrand et al., 2003; Orheim et al., 2023). While the Antarctic Coastal Current may transport icebergs calved at the Bellingshausen Sea/westernmost Antarctic Peninsula coasts to the Amundsen Sea Embayment shelf around Thurston Island and further west toward site PC493 (Mazur et al., 2019), the absence of <10 Ma old grains in PC493 during MIS 5, 11, and 15 argues against a significant contribution from these sources (Assmann et al., 2005), even though their contribution cannot be fully excluded. A sourcing of younger grains from Peter I. Island in the Bellingshausen Sea is also not likely. This island sits well within the ACC (Figure 1), which proxy records from the Atlantic sector of the Southern Ocean suggest was at a similar or more southerly position during past interglacials (Howe et al., 2002; Starr et al., 2025). Similarly, the eastern Victoria Land coast in the Ross Sea, where Miocene to Quaternary volcanic rocks crop out, is an unlikely source, because detritus from this region yields no biotite grains younger than 10 Ma but contains abundant 350–500 Ma old hornblende and biotite grains (Figure S1 in Supporting Information S1; cf. northern Victoria Land sector in Pierce et al., 2011), which are not observed at our sites.

An alternative origin for the young grains in MIS 5, 11, and 15 samples is the Marie Byrd Land volcanic province in the interior of the Wrigley Gulf-Hobbs Coast and Sulzberger Bay sectors. There, extensive young Miocene to Quaternary volcanic edifices crop out (Figure 3). Although predominantly hornblende, <10 Ma-old grains are also present in ice-proximal seafloor surface samples off the Wrigley Gulf-Hobbs Coast and Sulzberger Bay (Figure 3, Figure S1 in Supporting Information S1), and in basal debris from the Byrd Ice Core, in the southern part of the volcanic province (Marschalek et al., 2024; not investigated for biotite). Furthermore, icebergs calved from the Wrigley Gulf-Hobbs Coast and Sulzberger Bay sectors are readily transferred from the Antarctic Coastal Current into the ACC in the eastern Ross Sea (Figure 1; England et al., 2020). Taken together, these observations support a Marie Byrd Land volcanic province source for the young grains rather than the Antarctic Peninsula sector, even though the latter cannot be entirely excluded.

Glacial samples from core PS58/254 contain more grains with better-defined age population peaks, pointing to a more proximal source. The prominent 260 Ma peak of IRD in MIS 16 sediments strongly resembles the older age peak from the Thurston Island endmember. Additionally, the age spectrum of the MIS 12 sample is almost identical to the endmember from the Cosgrove Ice Shelf sector, while the MIS 6 and 10 samples contain age signatures resembling the Thurston Island endmember.

5.2. Latitudinal Shifts of the Southern ACC Boundary During Glacial-Interglacial Cycles

IRD provenance patterns differ markedly between the two core sites, with core PC493 showing exceptionally consistent IRD supply predominantly sourced from Thurston Island with variable contributions from the nearby ASE-W and the Pine Island Glacier-Thwaites Glacier sectors. In contrast, core PS58/254 exhibits systematic glacial-interglacial shifts; glacial sediments are characterized by exclusive IRD supply from southeastern sources (Thurston Island and Cosgrove Ice Shelf sectors), whereas interglacial sediments indicate additional IRD contributions from Marie Byrd Land (Wrigley Gulf-Hobbs Coast and Sulzberger Bay sectors). These provenance shifts likely reflect northward sbACC migration during glacial maxima, when the surface current direction switched from predominantly eastward to westward at site PS58/254, without influencing surface current flow at site PC493 (Figure 3). This interpretation is supported by sea-surface temperature and sea-ice reconstructions based on microfossil assemblages from the Pacific sector of the Southern Ocean, which indicate a 3–5° northward shift of ACC fronts (Southern ACC Front, Polar Front, and Subantarctic Front) during the last glacial period (Benz et al., 2016), and is consistent with a multi-proxy reconstruction of ACC flow variability during earlier

Quaternary glacials (Lamy et al., 2024). Our data indicate that this pattern of ACC frontal shifts and resulting provenance changes occurred consistently during all interglacial-glacial periods.

During pre-Holocene interglacials, ACC flow in the Pacific sector was likely stronger and its fronts positioned farther south (Lamy et al., 2024). This is consistent with observations for MIS 5, 11, and 15, where stronger ACC flow or a southward shift of the Southern ACC Front closer to site PS58/254 could have facilitated IRD transport from Marie Byrd Land to the core site. In this scenario, the sbACC must have remained north of site PC493, as no comparable provenance signal is observed there. Although similar ACC shifts occurred during other interglacials, provenance data indicate they were most pronounced during MIS 5, 11, and 15.

5.3. Implication for WAIS Dynamics Since the Mid-Pleistocene

IRD provenance changes between interglacials MIS 5, 11, and 15 and other interglacials at site PS58/254 cannot be interpreted as simply a change in source areas, because no potential source region bears <10 Ma grains in such a high abundance (Simões Pereira et al., 2018). Instead, this signature requires a change in the incorporation of glacigenic debris into the ice. Numerical modeling suggests that the ice-sheet elevation in central West Antarctica was significantly lower during MIS 5, 11, and 15 compared to MIS 17 and 19 (Sutter et al., 2019), likely lowering ice elevation along the Marie Byrd Land coast. There, WAIS thinning would have caused previously isolated nunataks to coalesce into mountain ranges drained by valley glaciers with exposed rock on their flanks. This environmental change would have promoted the production of supraglacial debris through erosion at the mountain flanks, rockfalls onto glacier surfaces and the formation of medial moraines (e.g., Scherler et al., 2018; Figure 3). Because Cenozoic volcanic rocks comprise most of the nunataks in interior Marie Byrd Land (Figure 3), this extra supraglacial debris would supply hornblende and biotite grains <10 Ma old. Furthermore, glaciers draining this thinner WAIS would have carried a greater proportion of supraglacial and englacial debris relative to basal debris compared to the modern ice sheet. Icebergs calving from such glaciers along the coast would have carried debris distributed throughout them, which would have taken longer to melt out.

All these processes could have increased the supply of glacigenic debris bearing <10 Ma old grains from the Marie Byrd Land volcanic province to the ocean, either via glaciers draining north to the Wrigley Gulf-Hobbs Coast and into Sulzberger Bay or via ice streams calving directly into the Ross Sea or feeding into the eastern Ross Ice Shelf. This detritus would eventually have been transported as IRD by icebergs that initially drifted within the Antarctic Coastal Current and were then entrained into the ACC, which transported them to site PS58/254. As noted above, the <10 Ma grains could also be explained by an Antarctic Peninsula source, but given the Marie Byrd Land contribution to the MIS 1 sediments, a Marie Byrd Land source is considered more likely. Even if some young grains originated from the Antarctic Peninsula, a similar ice-elevation–driven mechanism there would be required to explain their elevated proportion in the IRD deposited during these specific interglacials.

Because the provenance signature of glaciogenic debris supplied from the Pine Island Glacier-Thwaites Glacier sector closely matches that from the interior WAIS (i.e., Byrd Ice Core debris; cf. Figure S1 in Supporting Information S1), $^{40}Ar/^{39}Ar$ age distributions of IRD cannot reliably track grounded ice retreat in the Amundsen Sea drainage sector of the WAIS because such an upstream retreat would still result in the supply of grains with a similar age. However, the IRD record notably lacks distinctive provenance signals from the distal East Antarctic craton, such as Precambrian $^{40}Ar/^{39}Ar$ ages (>500 Ma) that occur in Dronning Maud Land (Pierce et al., 2014). Such a signal could be expected if an open-water seaway had developed between the Weddell and Amundsen Sea embayments (Vaughan et al., 2011), although high-resolution ocean modeling with a retreated WAIS would be required to verify this iceberg pathway. The absence of East Antarctic IRD may therefore argue for the continued cover of these seaways with an ice canopy, or even grounded ice, if the WAIS retreated substantially during the last 850 kyr. Recently, results of octopus DNA analyses had been interpreted to indicate the opening of seaways in response to WAIS collapse during MIS 5 (Lau et al., 2023), but sea-ice proxy data from an ice core in the Weddell Sea sector of the WAIS subsequently showed that the Ronne Ice Shelf had survived any WAIS retreat (Wolff et al., 2025). A diminished Ross Ice Shelf together with partial or full WAIS retreat during MIS 5 is suggested by dust provenance from a nearby ice core and modeled circulation changes (Carter et al., 2026). Our evidence for thinner ice in West Antarctica, without major shifts in provenance toward distinct East Antarctic sources, is consistent with a partial WAIS retreat during interglacial highstands over the past 850 kyr. Model simulations of a MIS 5 WAIS retreat consistent with our data indicate a sea-level contribution of under 3–4 m (Clark et al., 2020;

Golledge et al., 2021). This does not, however, exclude that during some interglacials only ice shelves remained over much of the region where the WAIS bed lies below sea level.

The changes in IRD supply from the Thurston Island and Cosgrove Ice Shelf sources in glacial samples from core PS58/254 also indicate a varying degree of glacial advance during these periods, likely reflecting the variable extent of individual ice stream advances. For instance, marine geophysical and sedimentological investigations showed that, in the easternmost ASE, the outer part of Abbot Trough, which had been eroded by a paleo-ice stream draining the Thurston Island and Cosgrove Ice Shelf sectors during past times of WAIS advance (Hochmuth & Gohl, 2013), had remained free of grounded ice during the last glacial period (Klages et al., 2017). Such an ice sheet configuration would have restricted the supply of glacigenic debris from Thurston Island to site PS58/254.

$^{40}Ar/^{39}Ar$ ages of hornblende, biotite, and mica from early Pliocene interglacial sediments at sites U1532 and U1533 (Passchier et al., 2025), located near site PS58/254, show distributions comparable to those at our sites, with most grains spanning 0–500 Ma (224/228 grains), as well as a peak at ∼90–100 Ma, and scattered ages between 140 and 300 Ma. This similarity indicates broadly consistent sediment provenance and transport pathways between the early Pliocene and Pleistocene interglacials, reflecting comparable ice-sheet and oceanographic configurations. However, the unimodal ∼170–180 Ma peak observed in Pliocene interglacial sediments, which is interpreted as evidence for large-scale WAIS retreat (Passchier et al., 2025), is absent at site PS58/254 (Figure S4 in Supporting Information S1). This absence may result from the limited sample resolution or the low grain abundance in interglacial sediments of our core. More likely, it indicates that WAIS retreat during Pleistocene interglacials was less extensive than during Pliocene interglacials.

Overall, our IRD provenance records reflect variability in ice sheet behavior and ocean circulation patterns in the Amundsen Sea during the last 850 kyr. At site PS58/254, glacial–interglacial shifts in IRD provenance reflect changes in ACC flow and latitudinal migration of the ACC front, while interglacial variations in IRD provenance are attributed to WAIS elevation changes influencing debris delivery from West Antarctica's interior. The persistent IRD provenance signal at site PC493, and the lack of East Antarctic signatures, suggest that parts of the WAIS remained grounded during interglacials of the last 850 kyr.

Conflict of Interest

The authors declare no conflicts of interest relevant to this study.

Availability Statement

The $^{40}Ar/^{39}Ar$ thermochronological data set used to trace different iceberg-rafted debris source areas in this study is archived in Zenodo (Hemming & Simões Pereira, 2026) and is available under a Creative Commons Attribution 4.0 International License.

Acknowledgments
P.S.P gratefully acknowledges support by the Kristian Gerhard Jebsen Foundation. J. W.M. and T.v.d.F. were funded by NERC Grants NE/W000172/1 and NE/X009394/1. We thank two anonymous reviewers for their constructive feedback, which greatly improved this manuscript. Open Access funding provided by Universitat Innsbruck/KEMÖ.

References

Assmann, K. M., Hellmer, H. H., & Jacobs, S. S. (2005). Amundsen Sea ice production and transport. *Journal of Geophysical Research*, *110*(C12). https://doi.org/10.1029/2004JC002797

Benz, V., Esper, O., Gersonde, R., Lamy, F., & Tiedemann, R. (2016). Last Glacial Maximum sea surface temperature and sea-ice extent in the Pacific sector of the Southern Ocean. *Quaternary Science Reviews*, *146*, 216–237. https://doi.org/10.1016/j.quascirev.2016.06.006

Carter, A. J., Aarons, S. M., Schnaubelt, J. C., Tabor, C. R., Higgins, J. A., Shackleton, S. A., et al. (2026). Diminished Ross Ice Shelf and West Antarctic Ice Sheet during Last Interglacial warming. *Nature Geoscience*, *19*(6), 1–8. https://doi.org/10.1038/s41561-026-01988-1

Clark, P. U., He, F., Golledge, N. R., Mitrovica, J. X., Dutton, A., Hoffman, J. S., & Dendy, S. (2020). Oceanic forcing of penultimate deglacial and last interglacial sea-level rise. *Nature*, *577*(7792), 660–664. https://doi.org/10.1038/s41586-020-1931-7

DeConto, R. M., & Pollard, D. (2016). Contribution of Antarctica to past and future sea-level rise. *Nature*, *531*(7596), 591–597. https://doi.org/10.1038/nature17145

Dorschel, B., Hehemann, L., Viquerat, S., Warnke, F., Dreutter, S., Tenberge, Y. S., et al. (2022). The international bathymetric chart of the southern ocean version 2. *Scientific Data*, *9*(1), 275. https://doi.org/10.1038/s41597-022-01366-7

England, M. R., Wagner, T. J. W., & Eisenman, I. (2020). Modeling the breakup of tabular icebergs. *Science Advances*, *6*(51), eabd1273. https://doi.org/10.1126/sciadv.abd1273

Golledge, N. R., Clark, P. U., He, F., Dutton, A., Turney, C. S. M., Fogwill, C. J., et al. (2021). Retreat of the Antarctic Ice Sheet during the last interglaciation and implications for future change. *Geophysical Research Letters*, *48*(17), e2021GL094513. https://doi.org/10.1029/2021GL094513

Hemming, S. R., & Simões Pereira, P. (2026). Downcore $^{40}Ar/^{39}Ar$ thermochronology of biotite and hornblende grains from Amundsen Sea sediment records during the late Pleistocene [Dataset]. *Zenodo*. https://doi.org/10.5281/ZENODO.20678528

Hillenbrand, C.-D., Grobe, H., Diekmann, B., Kuhn, G., & Fütterer, D. K. (2003). Distribution of clay minerals and proxies for productivity in surface sediments of the Bellingshausen and Amundsen seas (West Antarctica) – Relation to modern environmental conditions. *Marine Geology*, *193*(3), 253–271. https://doi.org/10.1016/S0025-3227(02)00659-X

Hillenbrand, C.-D., Kuhn, G., & Frederichs, T. (2009). Record of a mid-Pleistocene depositional anomaly in West Antarctic continental margin sediments: An indicator for ice-sheet collapse? *Quaternary Science Reviews*, *28*(13), 1147–1159. https://doi.org/10.1016/j.quascirev.2008.12.010

Hochmuth, K., & Gohl, K. (2013). Glaciomarine sedimentation dynamics of the Abbot glacial trough of the Amundsen Sea Embayment shelf, West Antarctica. *Geological Society, London, Special Publications*, *381*(1), 233–244. https://doi.org/10.1144/SP381.21

Holland, P. R., & Kwok, R. (2012). Wind-driven trends in Antarctic sea-ice drift. *Nature Geoscience*, *5*(12), 872–875. https://doi.org/10.1038/ngeo1627

Howe, J. A., Harland, R., & Pudsey, C. J. (2002). Dinoflagellate cyst evidence for Quaternary palaeoceanographic change in the northern Scotia Sea, South Atlantic Ocean. *Marine Geology*, *191*(1), 55–69. https://doi.org/10.1016/S0025-3227(02)00498-X

Jordan, T. A., Riley, T. R., & Siddoway, C. S. (2020). The geological history and evolution of West Antarctica. *Nature Reviews Earth & Environment*, *1*(2), 117–133. https://doi.org/10.1038/s43017-019-0013-6

Klages, J. P., Kuhn, G., Hillenbrand, C.-D., Smith, J. A., Graham, A. G. C., Nitsche, F. O., et al. (2017). Limited grounding-line advance onto the West Antarctic continental shelf in the easternmost Amundsen Sea Embayment during the last glacial period. *PLoS One*, *12*(7), e0181593. https://doi.org/10.1371/journal.pone.0181593

Konfirst, M. A., Scherer, R. P., Hillenbrand, C.-D., & Kuhn, G. (2012). A marine diatom record from the Amundsen Sea—Insights into oceanographic and climatic response to the Mid-Pleistocene Transition in the West Antarctic sector of the Southern Ocean. *Marine Micropaleontology*, *92–93*, 40–51. https://doi.org/10.1016/j.marmicro.2012.05.001

Lamy, F., Winckler, G., Arz, H. W., Farmer, J. R., Gottschalk, J., Lembke-Jene, L., et al. (2024). Five million years of Antarctic Circumpolar Current strength variability. *Nature*, *627*(8005), 789–796. https://doi.org/10.1038/s41586-024-07143-3

Lau, S. C. Y., Wilson, N. G., Golledge, N. R., Naish, T. R., Watts, P. C., Silva, C. N. S., et al. (2023). Genomic evidence for West Antarctic Ice Sheet collapse during the Last Interglacial. *Science*, *382*(6677), 1384–1389. https://doi.org/10.1126/science.ade0664

Marschalek, J. W., Blard, P.-H., Sarigulyan, E., Ehrmann, W., Hemming, S. R., Thomson, S. N., et al. (2024). Byrd ice core debris constrains the sediment provenance signature of central West Antarctica. *Geophysical Research Letters*, *51*(5), e2023GL106958. https://doi.org/10.1029/2023GL106958

Mazur, A. K., Wåhlin, A. K., & Kalén, O. (2019). The life cycle of small- to medium-sized icebergs in the Amundsen Sea Embayment. *Polar Research*, *38*. https://doi.org/10.33265/polar.v38.3313

Morlighem, M., Rignot, E., Binder, T., Blankenship, D., Drews, R., Eagles, G., et al. (2020). Deep glacial troughs and stabilizing ridges unveiled beneath the margins of the Antarctic ice sheet. *Nature Geoscience*, *13*(2), 132–137. https://doi.org/10.1038/s41561-019-0510-8

Orheim, O., Giles, A. B., Moholdt, G., Jacka, T. H., & Bjørdal, A. (2023). Antarctic iceberg distribution revealed through three decades of systematic ship-based observations in the SCAR international iceberg database. *Journal of Glaciology*, *69*(275), 551–565. https://doi.org/10.1017/jog.2022.84

Orsi, A. H., Whitworth, T., & Nowlin, W. D. (1995). On the meridional extent and fronts of the Antarctic Circumpolar Current. *Deep Sea Research Part I: Oceanographic Research Papers*, *42*(5), 641–673. https://doi.org/10.1016/0967-0637(95)00021-W

Passchier, S., Hillenbrand, C.-D., Hemming, S. R., Ehrmann, W., Frederichs, T., Bohaty, S. M., et al. (2025). West Antarctic ice retreat and paleoceanography in the Amundsen Sea in the warm early Pliocene. *Nature Communications*, *16*(1), 5609. https://doi.org/10.1038/s41467-025-60772-8

Pierce, E. L., Hemming, S. R., Williams, T., van de Flierdt, T., Thomson, S. N., Reiners, P. W., et al. (2014). A comparison of detrital U–Pb zircon, $^{40}Ar/^{39}Ar$ hornblende, $^{40}Ar/^{39}Ar$ biotite ages in marine sediments off East Antarctica: Implications for the geology of subglacial terrains and provenance studies. *Earth-Science Reviews*, *138*, 156–178. https://doi.org/10.1016/j.earscirev.2014.08.010

Pierce, E. L., Williams, T., van de Flierdt, T., Hemming, S. R., Goldstein, S. L., & Brachfeld, S. A. (2011). Characterizing the sediment provenance of East Antarctica's weak underbelly: The Aurora and Wilkes sub-glacial basins. *Paleoceanography*, *26*(4). https://doi.org/10.1029/2011PA002127

Rignot, E., Mouginot, J., Scheuchl, B., van den Broeke, M., van Wessem, M. J., & Morlighem, M. (2019). Four decades of Antarctic Ice Sheet mass balance from 1979–2017. *Proceedings of the National Academy of Sciences*, *116*(4), 1095–1103. https://doi.org/10.1073/pnas.1812883116

Roy, M., van de Flierdt, T., Hemming, S. R., & Goldstein, S. L. (2007). $^{40}Ar/39Ar$ ages of hornblende grains and bulk Sm/Nd isotopes of circum-Antarctic glacio-marine sediments: Implications for sediment provenance in the southern ocean. *Chemical Geology*, *244*(3), 507–519. https://doi.org/10.1016/j.chemgeo.2007.07.017

Scherer, R. P., Aldahan, A., Tulaczyk, S., Possnert, G., Engelhardt, H., & Kamb, B. (1998). Pleistocene collapse of the West Antarctic Ice Sheet. *Science*, *281*(5373), 82–85. https://doi.org/10.1126/science.281.5373.82

Scherler, D., Wulf, H., & Gorelick, N. (2018). Global assessment of supraglacial debris-cover extents. *Geophysical Research Letters*, *45*(21), 11798–11805. https://doi.org/10.1029/2018GL080158

Simões Pereira, P., van de Flierdt, T., Hemming, S. R., Frederichs, T., Hammond, S. J., Brachfeld, S., et al. (2020). The geochemical and mineralogical fingerprint of West Antarctica's weak underbelly: Pine Island and Thwaites glaciers. *Chemical Geology*, *550*, 119649. https://doi.org/10.1016/j.chemgeo.2020.119649

Simões Pereira, P., van de Flierdt, T., Hemming, S. R., Hammond, S. J., Kuhn, G., Brachfeld, S., et al. (2018). Geochemical fingerprints of glacially eroded bedrock from West Antarctica: Detrital thermochronology, radiogenic isotope systematics and trace element geochemistry in Late Holocene glacial-marine sediments. *Earth-Science Reviews*, *232*, 204–232. https://doi.org/10.1016/j.earscirev.2018.04.011

Spiegel, C., Lindow, J., Kamp, P. J. J., Meisel, O., Mukasa, S., Lisker, F., et al. (2016). Tectonomorphic evolution of Marie Byrd Land – Implications for Cenozoic rifting activity and onset of West Antarctic glaciation. *Global and Planetary Change*, *145*, 98–115. https://doi.org/10.1016/j.gloplacha.2016.08.013

Starr, A., Hall, I. R., Barker, S., Nederbragt, A., Owen, L., & Hemming, S. R. (2025). Shifting Antarctic Circumpolar Current south of Africa over the past 1.9 million years. *Science Advances*, *11*(1), eadp1692. https://doi.org/10.1126/sciadv.adp1692

Sutter, J., Fischer, H., Grosfeld, K., Karlsson, N. B., Kleiner, T., Van Liefferinge, B., & Eisen, O. (2019). Modelling the Antarctic Ice Sheet across the mid-Pleistocene transition – Implications for Oldest Ice. *The Cryosphere*, *13*(7), 2023–2041. https://doi.org/10.5194/tc-13-2023-2019

The RAISED Consortium, Bentley, M. J., Ó Cofaigh, C., Anderson, J. B., Conway, H., Davies, B., et al. (2014). A community-based geological reconstruction of Antarctic Ice Sheet deglaciation since the Last Glacial Maximum. *Quaternary Science Reviews*, *100*, 1–9. https://doi.org/10.1016/j.quascirev.2014.06.025

van Wyk de Vries, M., Bingham, R. G., & Hein, A. S. (2018). A new volcanic province: An inventory of subglacial volcanoes in West Antarctica. *Geological Society, London, Special Publications*, *461*(1), 231–248. https://doi.org/10.1144/SP461.7

Vaughan, D. G., Barnes, D. K. A., Fretwell, P. T., & Bingham, R. G. (2011). Potential seaways across West Antarctica. *Geochemistry, Geophysics, Geosystems*, *12*(10). https://doi.org/10.1029/2011GC003688

Williams, T. J., Hillenbrand, C.-D., Piotrowski, A. M., Allen, C. S., Frederichs, T., Smith, J. A., et al. (2019). Paleocirculation and ventilation history of southern ocean sourced deep water masses during the last 800,000 years. *Paleoceanography and Paleoclimatology*, *34*(5), 833–852. https://doi.org/10.1029/2018PA003472

Wolff, E. W., Mulvaney, R., Grieman, M. M., Hoffmann, H. M., Humby, J., Nehrbass-Ahles, C., et al. (2025). The Ronne Ice Shelf survived the last interglacial. *Nature*, *638*(8049), 133–137. https://doi.org/10.1038/s41586-024-08394-w

References From the Supporting Information

Dalrymple, G. B., Alexander, E. C., Jr., Lanphere, M. A., & Kraker, G. P. (1981). Irradiation of samples for $^{40}Ar/^{39}Ar$ dating using the Geological Survey TRIGA reactor (U.S. Geological Survey Professional Paper 1176).

Hillenbrand, C.-D., Fütterer, D. K., Grobe, H., & Frederichs, T. (2002). No evidence for a Pleistocene collapse of the West Antarctic Ice Sheet from continental margin sediments recovered in the Amundsen Sea. *Geo-Marine Letters*, *22*(2), 51–59. https://doi.org/10.1007/s00367-002-0097-7

Kuiper, K. F., Deino, A., Hilgen, F. J., Krijgsman, W., Renne, P. R., & Wijbrans, J. R. (2008). Synchronizing rock clocks of Earth history. *Science*, *320*(5875), 500–504. https://doi.org/10.1126/science.1154339

Lee, J.-Y., Marti, K., Severinghaus, J. P., Kawamura, K., Yoo, H.-S., Lee, J. B., & Kim, J. S. (2006). A redetermination of the isotopic abundances of atmospheric Ar. *Geochimica et Cosmochimica Acta*, *70*(17), 4507–4512. https://doi.org/10.1016/j.gca.2006.06.1563

Pankhurst, R. J., Millar, I. L., Grunow, A. M., & Storey, B. C. (1993). The pre-Cenozoic magmatic history of the Thurston Island Crustal Block, west Antarctica. *Journal of Geophysical Research*, *98*(B7), 11835–11849. https://doi.org/10.1029/93JB01157

Vermeesch, P. (2013). Multi-sample comparison of detrital age distributions. *Chemical Geology*, *341*, 140–146. https://doi.org/10.1016/j.chemgeo.2013.01.010